

## **Modeling of Energy-Autonomous and Sustainable Solar DTN Nodes and Their Impacts on the Performances of DTN Networks in the Context of Different Mobility Models and DTN Routing Protocols**



Sammou El Mastapha 

Department of Computer Science, Faculty of Sciences and Techniques, Cadi Ayyad University, Marrakesh 40000, Morocco

Corresponding Author Email: [sammou.elmastapha@yahoo.fr](mailto:sammou.elmastapha@yahoo.fr)

Copyright: ©2024 The author. This article is published by IIETA and is licensed under the CC BY 4.0 license (<http://creativecommons.org/licenses/by/4.0/>).

<https://doi.org/10.18280/ijepm.090402>

### **ABSTRACT**

**Received:** 29 February 2024

**Revised:** 10 August 2024

**Accepted:** 26 August 2024

**Available online:** 31 December 2024

#### **Keywords:**

*Delay-Tolerant Networks (DTN), mathematical and stochastic modeling, energy performance, solar DTN node, renewable energy sources, protocols, mobility model*

Delay-Tolerant Networks (DTN) are intermittent wireless mobile networks designed to handle communications in environments where network connectivity is often disrupted due to node mobility or the absence of fixed infrastructures. These frequent disconnections lead to repeated communication attempts between nodes, thereby increasing energy consumption. DTN is often deployed in isolated and hard-to-reach environments with limited energy sources, imposing significant constraints on the performance and operational lifetime of individual DTN nodes, as well as the DTN network as a whole. Despite the significant efforts invested by researchers to develop energy-efficient algorithms and models, the problem of energy consumption persists, especially with non-renewable sources. The motivation for this research is based on the major challenges related to powering mobile nodes in DTN networks, notably due to the absence of reliable and constant energy sources. The energy constraints of the nodes, combined with their mobility, raise problems of energy consumption and durability, leading to communication interruptions, delays, data losses, and a decrease in the overall efficiency of the network. To overcome these challenges, the article proposes a long-term energy management strategy by integrating renewable energy sources, notably solar energy, into the architecture of DTN nodes. The contributions include the modeling of an energy-autonomous and sustainable solar-powered DTN node, the evaluation of the energy generated and stored by these nodes, and the validation of the effectiveness of this approach through simulations in the ONE simulator, considering realistic mobility scenarios and communication conditions. The results show that solar DTN nodes have significantly higher residual energy than those with limited power sources. Additionally, social mobility models (MBM, SPMBM) consume more energy than individual models (RW, RWP, RD), while the Spray-and-Wait and PROPHET protocols are more energy-efficient compared to Epidemic and MaxProp. These analyses reveal optimal combinations of DTN protocols and mobility models to reduce energy consumption: the Spray-and-Wait protocol aligns well with social mobility models, while PROPHET is more suited to individual mobility models.

## **1. INTRODUCTION**

Delay-Tolerant Networks (DTNs) [1] are intermittent wireless mobile networks designed to handle communications in environments where network connections are intermittent due to node mobility or the absence of fixed communication infrastructures, presenting significant challenges. The frequency of disconnections in these networks, resulting from node mobility or other environmental factors, increases energy consumption, notably during repeated attempts to communicate between nodes.

The different routing approaches aim to optimize the performance of DTN networks by exploiting nodes characterized by high activities and significant energy consumption. Among these nodes, we find Cluster-Head (CH)

and Super Cluster-Head (SCH) [2], social nodes [3], and cooperative nodes [4]. However, any energy failure in these nodes leads to a noticeable deterioration in performance, highlighting the critical dependency of these nodes on their energy supply.

DTN nodes are often deployed in isolated and hard-to-reach environments [5, 6], such as remote, rural, disaster-stricken, or even extraterrestrial areas [7]. These environments impose significant energy constraints on nodes, equipped with limited energy sources such as small-capacity batteries or cells. In the face of these challenges, considerable efforts have been made to develop energy-efficient algorithms [8, 9], and models [10, 11]. However, the problem persists, especially when non-renewable energy sources are used.

The integration of renewable energy sources [12], such as

solar panels, seems to be a logical solution. These sources have seen notable expansion in recent years, with decreasing costs and increasing global adoption [13-15]. Despite progress, challenges persist due to the weight, size, and energy consumption constraints inherent in mobile devices. Initiatives such as the integration of solar panels into smartphones [16] illustrate advances toward more autonomous and sustainable communication devices, thereby reducing their dependence on traditional power sources.

The reduction in costs of solar technologies has also made these solutions more accessible for mobile network applications. The global adoption of solar renewable energy in communications equipment, including mobile nodes in computer networks, is part of a broader trend toward the sustainability of Information and Communication Technologies (ICTs).

To alleviate the routing problems and energy challenges associated with mobile nodes in DTN networks, we propose a long-term energy management strategy. This strategy involves integrating renewable energy sources, particularly solar energy, into the architecture of DTN nodes. This integration aims to improve the operational lifetime of DTN nodes while reducing their dependence on limited energy sources.

### 1.1 Motivation

The motivation behind our work stems from the significant challenges that DTN networks face in terms of powering mobile nodes, especially with unreliable energy sources. The combination of energy constraints with node mobility poses challenges in terms of energy consumption and sustainability, leading to communication interruptions, delays, and data losses. Isolated environments add significant constraints on the performance and operational lifetime of nodes.

Despite efforts to develop energy-efficient algorithms and models, energy consumption remains a major challenge, especially with non-renewable energy sources. The harnessing of renewable energy, particularly solar energy, offers a logical solution to these challenges, aligned with the global trend towards increasing adoption of renewable energy in communications.

### 1.2 Research objectives

One of the major challenges facing DTN networks is powering mobile nodes, especially in the absence of a reliable and constant power source. Mobile nodes often have energy constraints, and finding autonomous and renewable solutions is crucial for their sustainability. The main objectives of this research are as follows:

Proposing a long-term energy management strategy to address routing problems and energy challenges associated with mobile nodes in DTN networks.

Optimizing the choice of DTN protocols and mobility models in the context of renewable energy sources compared to the context of limited energy sources. The objective is to maximize the performance of DTN networks while taking into account the specificities of the energy sources used.

Developing a thorough understanding of the behaviors of DTN protocols in the contexts of renewable energy sources compared to contexts with limited energy sources. This understanding guides choices for the deployment and optimization of DTN networks, especially when renewable energy sources are involved.

### 1.3 Contributions

Our main contribution lies in the development of a long-term energy management strategy aimed at enhancing the sustainability and energy efficiency of mobile nodes in DTN networks. Our contributions include:

- The modeling of an energy-autonomous and energy-sustainable solar DTN node, including its renewable energy source and its main functional units.
- The mathematical modeling and evaluation of the energy power generated, as well as the amount of energy stored by a DTN node in regular movement and orientation, taking into account the daily solar cycle and geographical conditions.
- The stochastic modeling and evaluation of the energy power generated by a solar DTN node in random movement and orientation, taking into consideration the daily solar cycle and geographical conditions.

To validate the efficiency of our energy model in the context of DTN networks:

- We simulate our solar approach based on solar DTN nodes in the context of the ONE simulator, taking into account simulation scenarios that reflect realistic situations by adjusting the simulation parameters according to real-world communication conditions.
- We evaluate the impact of solar DTN nodes on the energy performance of DTN networks, compared to the impact of nodes with limited energy sources in the context of different DTN protocols and different mobility models, taking into account the average residual energy of nodes as a performance metric.

## 2. RELATED WORKS

Delay-Tolerant Networks (DTNs) [1] face crucial energy constraints due to the diversity of environments in which they operate. Mobile nodes or devices within these networks may be powered by limited energy sources, requiring efficient management of energy consumption to ensure continuous operation and extend the lifetime of the devices.

In these contexts, mobility models such as Random-Walk (RW) [17], Random-Waypoint (RWP) [18], Random-Direction (RD) [19], Map-Based-Movement (MBM) [20, 21], and Shortest-Path-Map-Based-Movement (SPMBM) [20, 21] play a crucial role in optimizing energy consumption. These models define the behavior of mobile nodes, thus influencing their movements, communication opportunities, and energy availability. Furthermore, the choice of DTN routing protocols, such as Epidemic [22], Prophet [23], Spray-and-Wait [24], and Maxprop [25], has a direct impact on the way messages are transmitted in the network, which has repercussions on energy consumption.

In addition to these mobility protocols and models, researchers have focused on developing strategies specifically designed to optimize energy consumption through energy-efficient algorithms [8, 9] and energy-efficient models [10, 11]. These approaches aim to address the energy constraints of DTN networks by proposing efficient mechanisms to manage and save the energy of mobile nodes.

Despite researchers' efforts to improve the energy efficiency of DTN networks, these initiatives are proving insufficient, notably in the face of battery energy consumption, which often depends on non-renewable energy sources. Despite

advancements in battery design that have not yet reached an optimal stage, these major challenges are prompting researchers to turn to the exploitation of renewable energy sources.

Piovesan et al. [26] explored the integration of renewable energy in next-generation mobile networks, particularly in the context of 5G technology, aiming to balance performance and sustainability. Khernane et al. [27] examined energy harvesting from renewable sources such as solar energy, vibrations, and radio frequencies to recharge sensors in wireless sensor networks (WSNs). Bouguera [28] proposed a multi-source energy harvesting system combining solar and wind energy to extend the lifespan of autonomous sensors.

The scarcity of studies and research focused on the integration of renewable energy resources in the context of DTN networks represents a significant gap in current research. While the field of DTN networks continues to evolve, few efforts have been dedicated to exploring and harnessing the advantages of renewable energies, especially solar energy. Renewable energy sources present a significant opportunity to improve the sustainability and resilience of DTN networks, but until now, this avenue has remained largely untapped.

It is imperative to conduct in-depth research in the field of DTN networks, with a focus on the integration of renewable energy resources, thus aligning these networks with the global trend towards increasing adoption of renewable energy in communications. The global adoption of solar renewable energies provides a unique opportunity to rethink how DTN networks are powered and operate, efficiently harnessing these clean and sustainable energy sources.

### 3. OUR APPROACHES FOR SOLAR-ENERGY DTN NETWORKS

#### 3.1 Discrete integration of solar systems in DTN nodes

DTN networks face energy challenges due to the mobility of the nodes and their limited autonomy, which impacts their performance. The integration of solar energy, among other renewable sources such as wind or kinetic energy, presents an effective solution. However, solar energy, in particular, proves to be the most appropriate and practical for DTN networks due to its availability and the ease of integrating solar panels onto mobile devices [28]. The proposed approach is to equip DTN nodes with discrete solar panels as shown in Figure 1, to capture solar energy and store it in energy storage systems, such as batteries, to maintain energy supply to the nodes even when solar energy is not available.



Figure 1. A solar DTN node [14]

This strategy ensures a continuous energy supply to the network nodes, thereby guaranteeing sustainable energy management and extending the lifespan of DTN networks.

#### 3.2 Architecture of a solar DTN node

The architecture of a solar node is designed to take into account the particular characteristics of DTN networks where communications can be intermittent, disconnected, or subject to significant delays. The basis of this architecture is based on powering the DTN node through the use of a renewable energy source, in particular solar energy. This power supply ensures the operation of three functional units, namely: The Processing Unit, the Memory Unit, and the Input/Output (I/O) Unit, as illustrated in Figure 2.

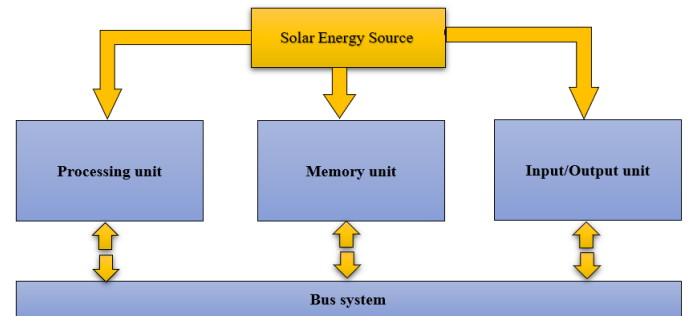


Figure 2. Architecture of a solar DTN node

- **Processing Unit:** This unit is responsible for managing the operations of the node. It performs functions such as processing bundles (data packets), managing queues, deciding on routing strategies, and overall control of the node. The processing unit can also handle decision-making for the storage, transmission, and routing of bundles.
- **Memory Unit:** The memory unit plays a central role in adapting DTN nodes to the challenging conditions of the network by providing buffer storage capacity to overcome delays, connectivity disruptions, and variations in resources. This unit is used to temporarily store bundles awaiting an opportunity for transmission.
- **Input/Output (I/O) Unit:** This is the interface that allows the DTN node to communicate with other nodes or with other external devices. The I/O unit is responsible for receiving bundles from other nodes and forwarding the bundles to other nodes. This unit also ensures interoperability with heterogeneous equipment in the context of new technologies.

These three units collaborate to ensure the optimal operation of DTN nodes, particularly in environments with intermittent or limited connectivity.

#### 3.3 Solar energy harvesting for a DTN node

##### 3.3.1 Importance of solar energy harvesting

Solar energy harvesting is crucial for a DTN node, particularly in isolated and hard-to-reach environments typical of DTN networks. By integrating solar panels, the DTN node can generate solar energy autonomously, providing a renewable energy source that decreases dependence on traditional and potentially limited sources. This approach significantly contributes to the energy efficiency of the DTN node, extending its operational lifetime and minimizing

interruptions due to energy shortages. Furthermore, solar energy harvesting also improves and strengthens the resilience and sustainability of the DTN network by ensuring continuous energy supply, even in conditions where other energy sources might be limited.

### 3.3.2 Solar energy harvesting cycle by a solar DTN node

The solar energy harvesting cycle of a DTN node is based on several key steps, contributing to its autonomy and reliability in mobile environments. This process begins with solar energy capture: the integrated solar panels use the photovoltaic effect [29] to convert light into energy through photovoltaic cells [29], specifically adapted for mobile use. Next, the charge controller regulates the energy flow to the batteries, using Maximum Power Point Tracking (MPPT) technology [30] to maximize charging under varying sunlight conditions. The energy stored in accumulators such as supercapacitors [31] or lithium-ion batteries [32] can then be used to power the node during periods without sunlight, as illustrated in Figure 3.

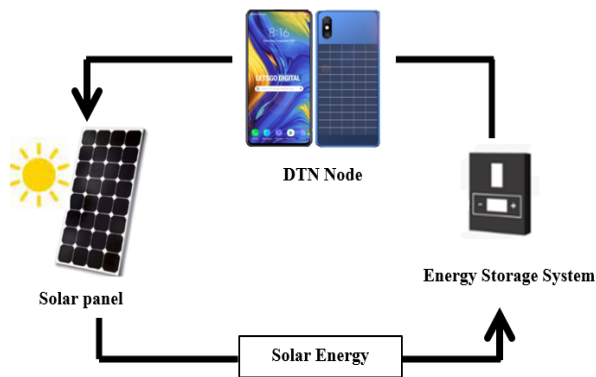


**Figure 3.** Solar energy harvesting cycle by a solar DTN node

Thus, during periods with no solar energy production, the stored energy powers the functional units of the DTN node, ensuring continuous power even in the absence of ideal lighting conditions, such as during the night or on cloudy days. Thus, solar energy harvesting contributes to the autonomy, durability, and reliability of the solar DTN node, ensuring its proper operation in mobile and intermittent environments where conventional charging is not practical.

## 4. MATHEMATICAL MODELING OF THE POWER GENERATED BY A SOLAR DTN NODE IN REGULAR MOVEMENT AND ORIENTATION

In this research work, we propose mathematical modeling that provides an estimate of the power generated by a solar DTN Node, taking into account the Solar time, the Solar Declination, the Solar Incidence Angle, the Solar Irradiance, Surface Area, and the Efficiency of the solar panel of the DTN node.

### 4.1 Modeling the solar time for a solar DTN node

Solar time ( $S_{time}$ ), also called solar time [33-35], is a time measurement based on the Sun's apparent position in the local sky relative to the meridian of the location under consideration. The Earth rotates about 15 degrees per hour, allowing solar

time to be modeled as a function of local time and geographic longitude with Eq. (1):

$$S_{time} = 15 \times (Local\ Time - 12) + Long \quad (1)$$

where,

- *Local Time*: Refers to the local time expressed in decimal hours (e.g., 13:30 = 13.5 hours).
- *(Local Time - 12)*: Adjusts the local time to account for local mean solar time by subtracting 12 hours.
- *15 × (Local Time - 12)*: Converts the adjusted time into degrees, with 15 degrees corresponding to one hour of Earth's rotation.
- *+Long*: We add the longitude of the location because the solar time angle also depends on the longitudinal position on the Earth.

### 4.2 Modeling the solar declination for a solar DTN node

The solar declination ( $S_{dec}$ ) [33-35] is the angle between the Sun's rays and the plane of the Earth's equator, as illustrated in Figure 4. It varies throughout the year due to the tilt of the Earth's rotational axis (approximately 23.5 degrees).

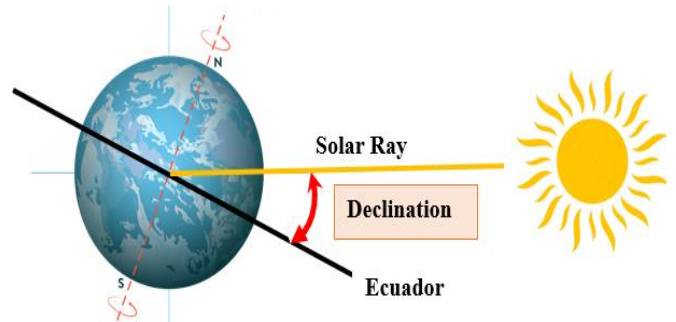


**Figure 4.** Solar declination for a solar DTN Node

The solar declination reaches its maximum positive value around June 21st (summer solstice) and its maximum negative value around December 21st (winter solstice). The declination is zero during the spring and autumn equinoxes, around March 21st and September 23rd. The expression for solar declination is given by Eq. (2):

$$S_{dec} = 23.5 \times \sin(360/365 \times (J - 81)) \quad (2)$$

where,

- *23.5 degrees*: Represents the Earth's average axial tilt.
- *360/365*: Used to adjust the calculation of the relative position in the year ( $J \in [1 \text{ to } 365]$ ), taking into account that the Earth completes a revolution in approximately 365 days.
- *J - 81*: Align the calculation with March 21, the day of the spring equinox, by considering that March 21 corresponds to  $J = 81$ .

### 4.3 Modeling the solar incidence angle for a solar DTN node

The solar incidence angle ( $I_A$ ) [36-38] is the angle between the sun's rays and a line perpendicular to the surface where the sunlight falls, as illustrated in Figure 5.

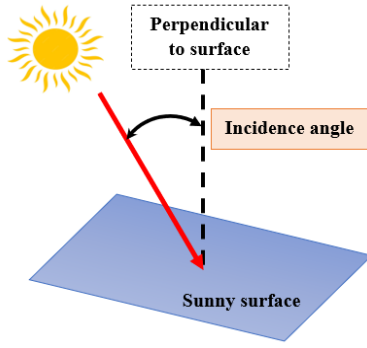


**Figure 5.** Solar incidence angle for a solar DTN node

This angle is essential for the efficiency of solar DTN nodes because a low incidence angle (solar rays perpendicular to the surface) allows for better solar energy capture. The solar incidence angle for a solar DTN node is expressed by Eqs. (3) and (4):

$$\cos(I_A) = \sin(Lat) \times \sin(S_{dec}) + \cos(Lat) \times \cos(S_{dec}) \times \cos(S_{time}) \quad (3)$$

$$I_A = \arccos(\sin(Lat) \times \sin(S_{dec}) + \cos(Lat) \times \cos(S_{dec}) \times \cos(S_{time})) \quad (4)$$

where,

- $S_{dec}$ : Solar\_Declination
- $S_{time}$ : Solar\_Time
- $Lat$ : Latitude
- $Long$ : Longitude

Optimizing the solar incidence angle is important for maximizing the efficiency of solar DTN nodes, as it allows more solar energy to be captured. This is especially important for solar DTN nodes where the amount of solar energy converted into stored energy depends directly on the angle of incidence.

#### 4.4 Modeling the solar irradiance for a solar DTN node

Solar Irradiance ( $G$ ): Solar irradiance [33, 35, 39-43] represents the energy per unit area collected from sunlight on the DTN node. It quantifies the incident solar power reaching the surface of a solar DTN node, typically measured in watts per square meter ( $W/m^2$ ). The solar irradiance can be calculated using Eq. (5):

$$G = G_{hor} \times \cos(I_A) \quad (5)$$

where,

- $G_{hor}$ : Solar Horizontal Irradiance
- $I_A$ : Solar Incidence Angle

The horizontal solar irradiance ( $G_{hor}$ ) serves as a reference to quantify the available solar energy in a given area, with an average value of  $1000 W/m^2$  under direct sunlight. However, this value can fluctuate depending on geographical and climatic conditions.

#### 4.5 Modeling the power generated by a solar DTN node

The power generated [35, 40, 43] by a solar DTN node represents the energy produced by the node's solar system. It is also a measure of the solar DTN node's capacity to convert

sunlight into usable energy. The generated power ( $P_{generated}$ ) is calculated using Eq. (6):

$$P_{generated} = G \times A_{panel} \times E_{panel} \quad (6)$$

where,

- $P_{generated}$ : Power generated by the solar DTN node (W),
- $A_{panel}$ : Solar panel area on the solar DTN node in ( $m^2$ ),
- $E_{panel}$ : Efficiency of the solar panel on solar DTN node (%),
- $G$ : Average solar Irradiance ( $W/m^2$ ).

This formula estimates the power generated under optimal conditions. It also provides insight into the solar panel's capacity to convert sunlight into power under these optimal conditions.

##### 4.5.1 Dimensions of a DTN solar node

The dimensions of the solar panel of the DTN Solar Node ( $A_{panel}$ ) influence the total quantity of energy captured. A larger surface area translates into greater energy capture. In our modeling approaches, we adopt a size commonly used in communication devices, corresponding to  $0.0136 m^2$  (see Figure 6).



**Figure 6.** Solar panel dimension of a solar DTN node

##### 4.5.2 Solar panel efficiency of a solar DTN node

The efficiency of a solar panel on a solar DTN node ( $E_{panel}$ ) measures the capacity of that node to convert solar energy into usable energy. This efficiency varies depending on the type of solar panel and the manufacturer, with efficiencies generally between 15% and 22%. However, notable progress has been made, such as the world record set by Fraunhofer ISE [44], with a conversion efficiency of 36.1% for multi-junction solar cells.

Moreover, recent studies, such as the one presented in study [45], emphasize the importance of optimizing the performance of photovoltaic systems through approaches that include fault detection and mitigation to maximize energy production. Research [46] also demonstrates that the efficiency of photovoltaic systems can be enhanced by using cooling systems, which help maintain optimal panel temperatures and improve energy yield. Furthermore, other studies [47] highlight that the efficiency of solar panels can be influenced by environmental factors, such as dust accumulation on the panels, which can significantly reduce their efficiency.

#### 4.6 Modeling the energy stored by a solar DTN node

The stored energy [48] in the battery of a solar DTN node is estimated using Eq. (7):

$$E_{St} = P_{generated} \times T_{exp} \quad (7)$$

where,

- $E_{St}$  represents the stored energy in joules,
- $P_{generated}$  is the power generated by the solar DTN node in watts,
- $T_{exp}$ : Exposure time of the solar DTN node to the sun in seconds.

This formula provides an estimate of the total stored energy based on the power generated and the duration of sun exposure. However, it does not account for energy losses due to various factors such as battery efficiency, losses in cables and components, and environmental conditions.

#### 4.7 Modeling the energy consumed by a solar DTN node

The mathematical modeling of energy consumption by a solar DTN node depends on several factors that contribute to energy consumption, including the functional units of the DTN node, the communication mode, the DTN protocols used, the communication activities of the Solar DTN node, etc. However, a general approach can be developed by focusing on aspects commonly used in DTN networks, such as transmission, reception, and relay node search. The fundamental formulation of the energy consumption of a Solar DTN node is given by Eq. (8):

$$C_{DTN} = P_{DTN} \times T \quad (8)$$

where,

$C_{DTN}$  is the energy consumed during the communication activity of the DTN node,  $P_{DTN}$  is the power of the communication activity of the Solar DTN node, and  $T$  is the activity time, representing the duration during which the node is active and performs communication operations.

##### 4.7.1 Energy consumption during transmission

The energy consumption during transmission mainly depends on the transmission power and transmission time. We can model this mathematically as follows:

$$C_{transmission} = P_{transmission} \times T_{transmission} \quad (9)$$

where,

$C_{transmission}$  is the energy consumed during transmission,  $P_{transmission}$  is the transmission power, and  $T_{transmission}$  is the transmission time.

##### 4.7.2 Energy consumption during reception

The energy consumption during reception depends on the

receiving power and the reception time. The modeling can be similar to that of transmission:

$$C_{reception} = P_{reception} \times T_{reception} \quad (10)$$

where,

$C_{reception}$  is the energy consumed during reception,  $P_{reception}$  is the reception power, and  $T_{reception}$  is the reception time.

##### 4.7.3 Energy consumption during relay node search

The energy consumption during the search for a relay node depends on the search power and the search time. We can model this mathematically in the same way:

$$C_{search} = P_{search} \times T_{search} \quad (11)$$

where,

$C_{search}$  is the energy consumed during the search,  $P_{search}$  is the search power, and  $T_{search}$  is the search time.

## 5. MATHEMATICAL EVALUATION OF THE POWER GENERATED BY A SOLAR DTN NODE IN REGULAR MOVEMENT AND ORIENTATION

To evaluate our mathematical modeling approach, we will choose a geographical location in Marrakech, Morocco (Latitude: 31.6341600°, Longitude: -7.9999400°), and we will consider a specific sunny day starting from 08h00 (8 a.m.) to 17h00 (5 p.m.), for example, June 21, the day of the summer solstice, which corresponds to day 172 of the year.

During a sunny day, we will carefully analyze variations in solar time ( $S_{time}$ ), solar declination ( $S_{dec}$ ), solar incidence angle ( $I_A$ ), solar irradiance ( $G$ ), and generated power ( $P_{generated}$ ), along with the amount of stored energy ( $E_{St}$ ) in a solar DTN node. This analysis will be conducted in correlation with the apparent trajectory of the sun in the sky, which changes based on the time of day. Table 1 below presents the evolution of solar characteristics for a solar DTN node for each hour during day 172 of the year, from 8:00 (8 a.m.) to 17:00 (5 p.m.). It includes calculations for solar time ( $S_{time}$ ), solar declination ( $S_{dec}$ ), solar incidence angle ( $I_A$ ), solar irradiance ( $G$ ), generated power ( $P_{generated}$ ), and the amount of stored energy ( $E_{St}$ ) by the solar DTN node. These calculations are performed using modeling equations and correspond to precise periods of a sunny day.

**Table 1.** Evolution of solar characteristics for a solar DTN node

Local Time	$S_{time}$	$S_{dec}$	$I_A$	$G$	$P_{generated}$
8:00	-1.18682	0.40044	1.049342	498.14166	1.35494
9:00	-0.92502	0.40044	0.828054	676.31031	1.83956
10:00	-0.66322	0.40044	0.60532	822.31821	2.23670
11:00	-0.40142	0.40044	0.38655	926.21518	2.51930
12:00	-0.13962	0.40044	0.19565	980.92080	2.66810
13:00	0.12217	0.40044	0.18624	982.70698	2.67296
14:00	0.38397	0.40044	0.37241	931.45199	2.53354
15:00	0.64577	0.40044	0.59052	830.64877	2.25936
16:00	0.90757	0.40044	0.81321	687.16690	1.86909
17:00	1.16937	0.40044	1.03469	510.78443	1.38933

### 5.1 Solar time

Solar time ( $S_{time}$ ) is based on the position of the sun in the sky, and this position changes throughout the day using solar noon as a reference. Solar noon represents the moment when the sun reaches its highest position in the sky, corresponding to the almost zero-hour angle (local time is 12 p.m.). After solar noon, solar time increases as the sun moves toward the western horizon. This means that, on a normal day, solar time increases after 12:00 local time. This variation is expected. The increase in solar time with local time is consistent with the apparent movement of the Sun across the sky during the day (see Figure 7).

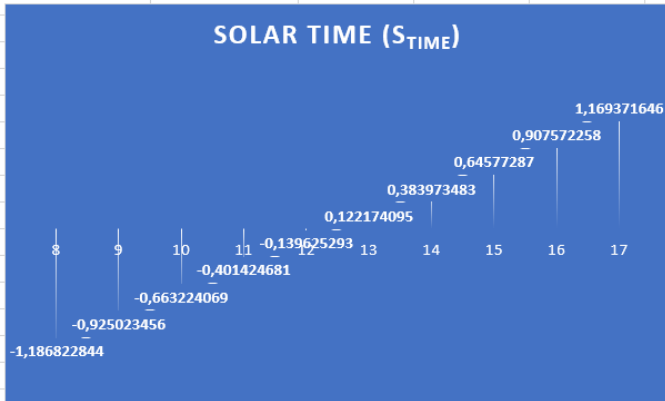


Figure 7. Solar time of a solar DTN node

### 5.2 Solar incidence angle

The solar incidence angle of a solar DTN node varies throughout the day depending on the position of the sun. At sunrise, the angle is low, resulting in greater dispersion of the solar rays and a decrease in light intensity. At noon, the angle is minimal, maximizing light intensity and solar energy production. At sunset, the angle increases again, reducing light intensity as the rays traverse a greater thickness of the atmosphere (see Figure 8).

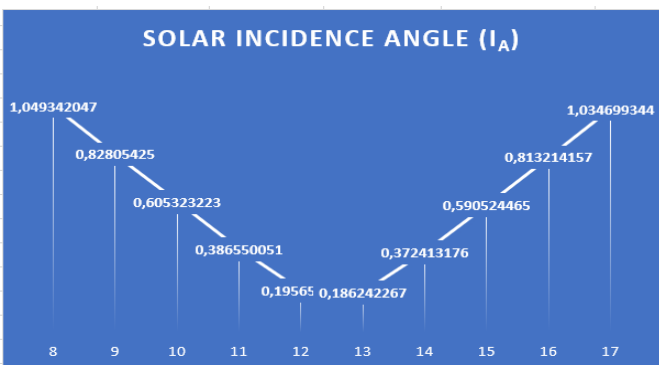


Figure 8. Solar incidence angle of a solar DTN node

### 5.3 Solar irradiance

The solar irradiance of a solar DTN node varies throughout the day depending on the position of the sun. At sunrise, the irradiance is low due to the thick atmosphere the solar rays' traverse, as well as an oblique incidence angle. At noon, the irradiance reaches its maximum when the sun is at its highest point in the sky, and the sun's rays are nearly perpendicular to

the Earth's surface, thus maximizing the solar energy received. In the late afternoon and sunset, the irradiance decreases as the sun descends toward the horizon. The incidence angle becomes more oblique, further dispersing the solar energy and thereby reducing the irradiance (see Figure 9).

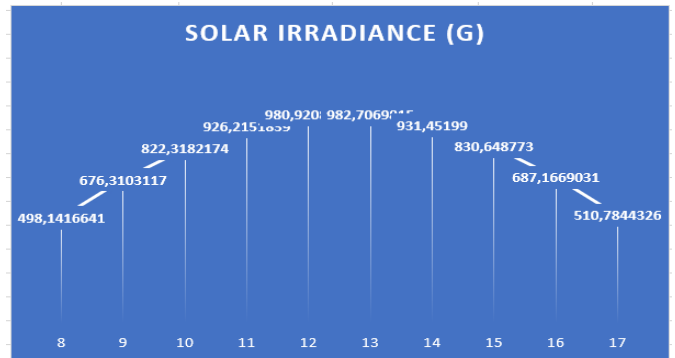


Figure 9. Solar irradiance of a solar DTN node

### 5.4 Power generated

During a sunny day, the power generated by a Solar DTN Node tends to be lower at sunrise, peaks around solar noon, and then decreases again at sunset. This variation is mainly due to the angle of solar incidence, which influences the amount of solar energy reaching the solar DTN nodes (see Figure 10).



Figure 10. Power generated by a solar DTN node

### 5.5 Energy storage

The amount of stored energy can vary depending on the duration of exposure to sunlight throughout the day. Table 2 below shows the variation and evolution of the energy stored in a solar DTN node as a function of the power generated during each hour.

Table 2. Evolution of energy stored by a solar DTN node

Local Time	$P_{generated}$	$E_{St}$
8:00-9:00	1,354,945,326	4877,803,175
9:00-10:00	1,839,564,048	6622,430,572
10:00-11:00	2,236,705,551	8052,139,985
11:00-12:00	2,519,305,51	9069,499,08
12:00-13:00	2,668,104,588	9605,176,517
13:00-14:00	2,672,962,999	9622,666,763
14:00-15:00	2,533,549,413	9120,777,886
15:00-16:00	2,259,364,663	8133,712,785
16:00-17:00	1,869,093,976	6728,738,315
17:00-18:00	1,389,333,657	5001,601,164

These data are crucial for optimizing the use of solar DTN nodes. They allow for determining the periods of the day when energy production and storage are most effective, which can guide decisions in energy planning and management. Figure 11 below shows the evolution of the quantity of stored energy as a function of solar exposure during each hour of the day.

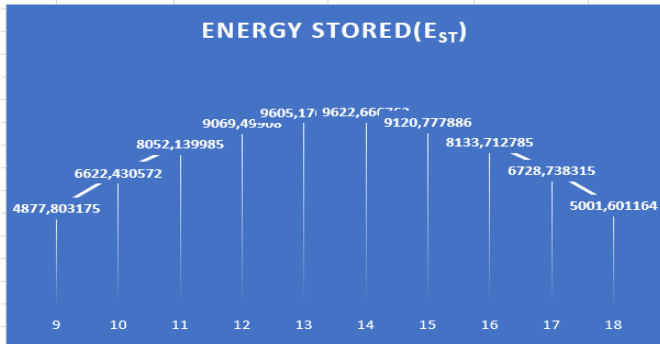


Figure 11. Energy stored by a solar DTN node

On a sunny day, the amount of energy stored in a solar DTN node's battery is lowest at sunrise due to the solar incidence angle and the sun's position. It reaches its maximum around solar noon, when solar power is at its peak, allowing for optimal battery charging. At the end of the day, the amount of energy stored decreases as the sun moves toward the horizon, reducing the battery charge.

## 6. STOCHASTIC MODELING OF THE POWER GENERATED BY A SOLAR DTN NODE IN RANDOM MOVEMENT AND ORIENTATION

The modeling of the solar incidence angle, solar irradiance, and generated power becomes more complex when the solar DTN node exhibits random movements and orientations. This complexity is further increased by the constant variations in the position of the sun.

The adoption of a simulation approach, such as the Monte Carlo method [49], can be particularly relevant in the context of DTN networks where the movements of solar DTN nodes and their orientation changes over time are often unpredictable and random. The Monte Carlo method is a stochastic technique based on the simulation of multiple possible scenarios to estimate probabilistic outcomes.

In the context of a solar DTN node with random orientations, we can use the Monte Carlo method to obtain a probabilistic estimate of the solar incidence angle ( $I_A$ ), solar irradiance ( $G$ ), and generated power ( $P_{generated}$ ).

### 6.1 Monte Carlo approach for solar DTN nodes

The Monte Carlo approach adapted to the context of a solar DTN node with random orientations involves several essential steps, namely:

#### 1) Step 1: Define Random Variables

We define three uniformly distributed random variables: the orientation of the solar DTN node (orientation), solar declination ( $S_{dec}$ ), and solar time ( $S_{time}$ ).

#### 2) Step 2: Sample Generation

We generate random samples uniformly for each variable. These samples represent possible scenarios for the solar DTN

node.

- The random variable 'Orientation': Samples are generated between 0 and 360 degrees.
- The random variable 'Solar Declination': Samples are generated between -23.5 and 23.5 degrees.
- The random variable 'Solar Time': Samples are generated between 0 and 24 hours.

#### 3) Step 3: Calculation of Solar Incidence Angle ( $I_A$ ), Solar Irradiance and Generated Power

We use the generated samples to calculate the solar incidence angle ( $I_A$ ), solar irradiance, and generated power by the solar DTN node as a function of the orientation, solar time, and solar declination. Additionally, we convert the incidence angles from radians to degrees.

#### 4) Step 4: Repetition of the Process

We repeat steps 2 and 3 a large number of times (number of iterations = 1000) to obtain a statistical distribution of possible results. This makes it possible to obtain a probabilistic estimate of the power generated by the solar DTN node as a function of the variables considered.

#### 5) Step 5: Analysis of Results

We analyze the distribution of results obtained to understand the variability and uncertainty associated with the solar incidence angle, solar irradiance, and generated power.

#### 6) Step 6: Estimation of the Mathematical Expectation of the Results

The expected value of the solar incidence angle, the solar irradiance, and the generated power by a solar DTN node are estimated by taking the weighted average of the calculated values over the generated samples.

### 6.2 Monte Carlo simulation algorithm for a solar DTN node

The Pseudo-Code algorithm for the Monte Carlo simulation, adapted to the context of a solar DTN node with random orientations, is designed as follows:

<p><b>Algorithm:</b> Monte Carlo Simulation Algorithm for a Solar DTN Node</p> <p><b>Input:</b> orientation, solar_declination, solar_time,  # Constant horizontal irradiance  <math>G_{horizontal} = 1000</math>,  # Constant Panel Efficiency  <math>E_{panel} = 0.2</math>,  # Constant Panel Dimensions  <math>A_{panel} = 0.0136</math></p> <p><b>Output:</b> <math>I_A</math>, <math>G</math>, <math>P_{generated}</math>,  # A list of generated solar incidence angles  list_incidence_angles = [],  # A list of generated solar irradiances  list_irradiances = [],  # A list of generated powers  list_generated_powers = []</p> <p><b>For</b> i from 1 to numberOfSamples:  # Generate random parameters  orientation ← GenerateRandomNumberBetween(0, 360);  solar_declination ← GenerateRandomNumberBetween(-23.5, +23.5);  solar_time ← GenerateRandomNumberBetween(0, 24);  # Calculation of solar incidence angle</p>
---

```

IA ← arccos[sin(solar_declination) *
sin(orientation) + cos(solar_declination) *
cos(orientation) * cos(solar_time)];
# Calculation of solar irradiance
G ← G_horizontal * cos(IA);

# Calculation of generated power
P_generated ← G * A_panel * E_panel;
# Adding results to lists
list_incidence_angles.append(IA);
list_irradiances.append(G);
list_generated_powers.append(P_generated);
End_For
# Analysis of results
PlotHistogram(list_incidence_angles, "Solar Incidence
Angles");
PlotHistogram(list_irradiances, "Solar Irradiance");
PlotHistogram(list_generated_powers, "Generated
Power";

```

## 7. STOCHASTIC EVALUATION OF THE POWER GENERATED BY A SOLAR DTN NODE IN RANDOM MOVEMENT AND ORIENTATION

### 7.1 Solar incidence angle

Figure 12 represents the histogram of the solar incidence angle as a function of the probability density. In the context of our Monte Carlo simulation, the probability density of a solar DTN node with random orientations represents the probability of observing different values of the solar incidence angle. Angle ranges with higher probability densities indicate the most frequently observed values in the samples. The incidence angle distribution diagram helps identify the regions of interest where the probability density is significant, as shown in Table 3.

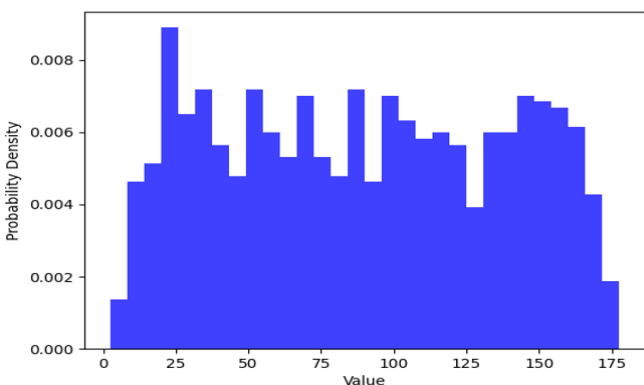


Figure 12. Solar incidence angle distribution

Table 3. Range of interest for the solar incidence angle

Range of Interest for the Solar Incidence Angle	High Probability Density
[20, 25]	0.009
[35, 40]	0.007
[50, 55]	0.007
[65, 70]	0.0068
[85, 90]	0.007
[95, 100]	0.0068
[145, 150]	0.0068

To deduce the suitable solar incidence angle for a solar DTN node with random orientations by calculating the weighted average of the solar incidence angles using the probability density as weights, as shown in Eq. (12):

$$\text{Average Incidence Angle} = \frac{\sum(\text{Incidence Angle}_i \times \text{probability}_i)}{\sum \text{probability}_i} \quad (12)$$

As long as we have ranges of solar incidence angles and not specific values, the weighted average can be approximated by using the center of each range as a representative value. This is often done by assuming that the distribution of the solar incidence angle is relatively uniform within each range.

The obtained value ( $\approx 70.83333333$ ) represents an estimate of the average solar incidence angle weighted by the probability associated with each range. This can be interpreted as the expected average incidence angle value considering the probability distribution within these ranges.

### 7.2 Solar irradiance

Solar irradiance varies depending on the position of the sun and atmospheric conditions (see Figure 13). It decreases significantly as the solar incidence angle approaches 90 degrees, becoming almost zero at this angle. In our Monte Carlo simulation, negative solar irradiance is considered null, particularly when the incidence angle significantly reduces sunlight on the surface of the solar DTN node, causing a shadow projection that reduces irradiance to negative values. The analysis of solar irradiance distribution through the histogram allows the identification of areas of interest with high probability density, summarized in Table 4.

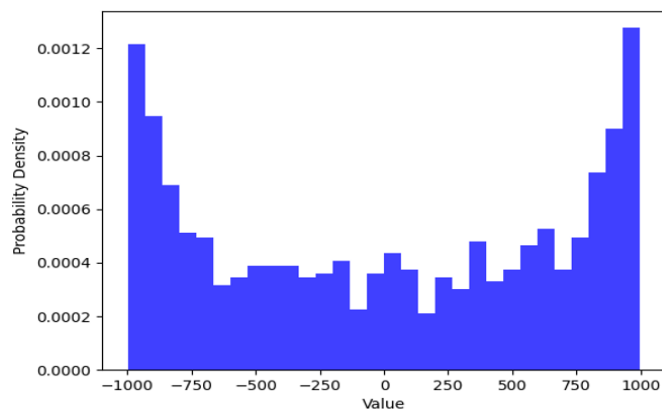


Figure 13. Solar irradiance distribution

Table 4. Range of interest for solar irradiance

Solar Irradiance Range of Interest	High Probability Density
[0, 500]	0.00042
[300, 350]	0.00048
[600, 650]	0.00044
[650, 700]	0.00053
[750, 800]	0.0005
[800, 850]	0.00075
[900, 950]	0.0009
[950, 1000]	0.00128

To determine the appropriate solar irradiance for a solar DTN node with random orientations, one proceeds by

calculating the weighted average of the solar irradiances using the probability density as a weighting factor, as shown in Eq. (13):

$$\text{Average Irradiance} = \frac{\sum(\text{Irradiance}_i \times \text{probability}_i)}{\sum \text{probability}_i} \quad (13)$$

When solar irradiance values are defined by ranges rather than specific values, it is possible to approximate the weighted average by using the center of each range as a representative value. This approximation is often based on the assumption of a relatively uniform distribution of solar irradiance within each range.

The resulting value ( $\approx 751.0377358$ ) represents an estimation of the weighted average irradiance by the probability associated with each range. This estimation can be interpreted as the expected value of the average irradiance, considering the probability distribution within these ranges.

### 7.3 Generated power

The power generated by a solar DTN node naturally varies based on the sun's trajectory and atmospheric conditions (see Figure 14). It is generally minimal at sunrise, reaches its peak around solar noon, and then gradually decreases until sunset. In the context of our Monte Carlo simulation, the negative powers can be considered as zero, especially when a high solar incidence angle, such as at sunrise or sunset, leads to a substantial reduction in solar illuminance on the surface of the solar DTN node. These negative values represent nighttime and the absence of solar rays. By analyzing the distribution of the generated power on the diagram, we can identify ranges of interest with higher probability density. Table 5 groups the ranges of generated power of interest, characterized by high probability density.

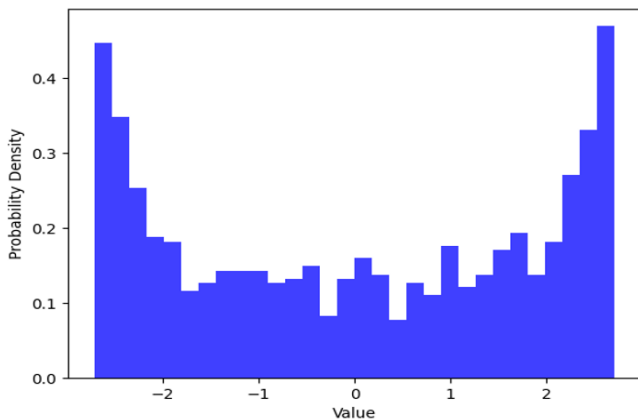


Figure 14. Generated power distribution

Table 5. Range of interest for generated power

Range of Interest for Generated Power	High Probability Density
[0, 0.2]	0.16
[0.8, 1]	0.175
[1.4, 1.6]	0.17
[1.6, 1.8]	0.195
[2, 2.2]	0.18
[2.2, 2.4]	0.27
[2.4, 2.6]	0.33
[2.6, 2.8]	0.48

The ranges of generated power with high probability densities are more likely in our Monte Carlo simulation.

To estimate the appropriate generated power for a solar DTN node with random orientations, the weighted average of the generated powers is calculated using the probability density as the weighting coefficient, as shown in Eq. (14):

$$\text{Average Generated Power} = \frac{\sum(\text{Generated Power}_i \times \text{probability}_i)}{\sum \text{probability}_i} \quad (14)$$

The resulting value (approximately 1.97959184 watts) is an estimate of the probability-weighted average generated power associated with each range. This estimate can be interpreted as the expected value of the average generated power, taking into consideration the probability distribution within these ranges.

## 8. SIMULATION ENVIRONMENT AND CONFIGURATION

In this research, the ONE simulator (Opportunistic Network Environment) [21, 50] was used to simulate solar-based approaches and evaluate the energy performance of solar and ordinary DTN nodes, considering DTN protocols and mobility models. The ONE simulator integrated an energy module [50] to model the energy consumption and management of nodes. This module simulates operations such as message transmission, reception, and power transitions, providing researchers with a valuable tool for analyzing the energy performance of protocols and algorithms in environments with intermittent connectivity.

### 8.1 Configuring renewable energy in the ONE simulator

We have configured the ONE simulator's energy system to account for sustainable solar energy. This configuration involves adding a solar energy source to each solar DTN node, with the capacity to adjust the recharge frequency of the nodes depending on this energy source. The solar energy mechanism has been integrated directly into the ONE simulator routing system, as shown in Figure 15.

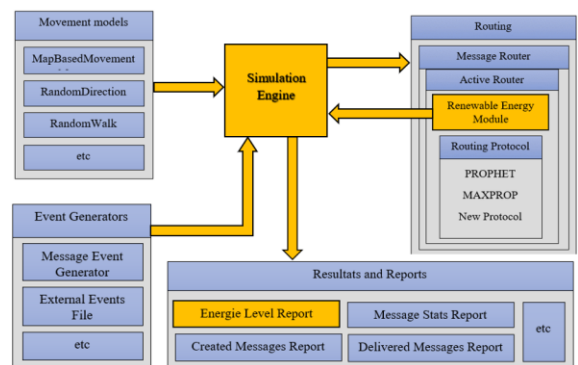


Figure 15. Configuring renewable energy in the ONE simulator

This configuration also allows for a more realistic simulation of the energy performance of DTN nodes, taking into account variations in solar energy and the associated battery recharge during the day.

Depending on the configuration, the amount of solar energy

recharged in the DTN node battery varies according to the daily solar cycle, taking into account sunny days. Table 6 below shows the evolution of the battery recharge of a solar DTN node throughout the day.

**Table 6.** Evolution of recharge in a solar DTN node

Recharge Interval	Amount of Recharged Energy
8h00-9h00	4877,803175
9h00-10h00	6622,430572
10h00-11h00	8052,139985
11h00-12h00	9069,49908
12h00-1300	9605,176517
13h00-1400	9622,666763
14h00-15h00	9120,777886
15h00-16h00	8133,712785
16h00-1700	6728,738315
17h00-18h00	5001,601164

By integrating this functionality, our approach is aimed at more precisely evaluating the impact of renewable energy sources, in particular solar energy, on the energy performance of DTN nodes. This should contribute to a better understanding of real-world scenarios and varying conditions that DTN networks may face.

## 8.2 Simulation parameters

This section describes the simulation parameters used to evaluate the impact of solar DTN nodes on the performance of DTN networks. The simulations incorporate various routing protocols (Epidemic, Prophet, Spray-and-Wait, MaxProp) as well as several mobility models, including individual random models (RW, RWP, RD) and map-based social models (MBM, SPMBM). Table 7 summarizes the simulation parameters.

**Table 7.** DTN simulation settings

Configuration Setting	Value
Simulation Duration	25000 seconds
Network Area Size	4500 meters by 3400 meters
DTN Routing Strategy	Epidemic, Prophet, Spray- and - Wait, and MaxProp
Node Movement Models	RW, MBM, RWP, SPMBM, RD
Buffer Capacity	5 MB (Megabytes)
Waiting Time	0–120 seconds
Node Movement Speed	0.5 m/s to 1.5 m/s
Spray-and-Wait Copy Limit	L (Number of Copies) = 10
Data Transmission Speed	2 Mbps equivalent to 250 kB/s)
Message Time-To-Live	300-minute period
Communication Range	A distance of 10 meters
Message Generation	One New Message every 25–35 seconds
Message Volume	500 kB to 1 MB
Energy Storage Capacity	9600 J (Joules)
Starting Energy	4800 J (joules)
Ordinary DTN Node Recharge Frequency	13.89 hours (50,000 seconds)
Solar DTN Node Recharge Frequency	1 hour (3600 seconds)
Data Transmission Energy	0.08 J (Joules)
Data Reception Energy	0.08 J (Joules)
Relay Node Search Energy	0.08 J (Joules)

The nodes have an initial energy budget of 4800 joules, with energy costs for transmitting (0.08 joules), receiving (0.08 joules), and searching for relays (0.92 joules). The solar nodes recharge their energy based on sun exposure, with a recharge

time of 3600 seconds (one hour). The amount of energy recharged by a solar node depends on the time of day, the duration of sun exposure, and geographical conditions, as illustrated in Table 6. On the other hand, nodes with limited energy have a recharge time of 50,000 seconds, which exceeds the total duration of the simulation. These parameters aim to reproduce the real communication conditions of DTN networks, taking into account mobility, routing protocols, energy management, and the recharging characteristics of solar nodes.

## 9. SIMULATION RESULTS AND DISCUSSION

In this section, we present the results of simulations performed using the ONE simulator. We compare the energy performance of solar DTN Nodes exploiting renewable energy resources with those of DTN nodes using limited energy resources.

### 9.1 Performance metric

The average residual energy expressed in joules (J), serves as an essential metric in DTN networks. It indicates the remaining energy in the network nodes' batteries after a given duration of operation or simulation. This metric reflects the available energy for node activities such as transmitting and receiving data, searching for relay nodes, and managing mobility, among other tasks.

### 9.2 Evaluation of the energy performance of solar DTN nodes using renewable energy resources

In this section, we evaluate the energy performance of solar DTN nodes equipped with renewable energy resources, considering different mobility models (MBM, SPMBM, RW, RWP, RD) and routing protocols (Epidemic, Prophet, Spray-and-Wait, MaxProp), while varying node density. Figures 16-20 illustrate the energy performance of solar DTN nodes in terms of residual energy, depending on mobility models and routing protocols.

#### 9.2.1 Residual energy

The analysis of the results shows that the average residual energy of solar DTN nodes, evaluated using the DTN protocols, significantly exceeds the initial energy of 4800 Joules. The random models (RW, RWP, RD) maintain high levels of residual energy, reaching 8881.72 Joules, 8879.09 Joules, and 8879.65 Joules, respectively. In contrast, the map-based models (MBM, SPMBM) exhibit lower levels of residual energy, reaching 8857.86 Joules and 8828.83 Joules, respectively. These variations can be primarily explained by the characteristics of the mobility models and the routing strategies adopted by the nodes, which influence energy consumption.

#### 9.2.2 Energy consumption

The energy consumption of the nodes is strongly influenced by the mobility models and the adopted protocols. The random models, such as RW, RWP, and RD, consume 718.275382 Joules, 720.905129 Joules, and 720.349807 Joules, respectively. These models are characterized by less frequent transmissions, resulting in more efficient energy management. In contrast, the map-based models, such as MBM and SPMBM,

show higher energy consumption, reaching 742.13414 Joules and 771.162075 Joules, respectively, due to more directed movements and additional calculations to optimize the routes.

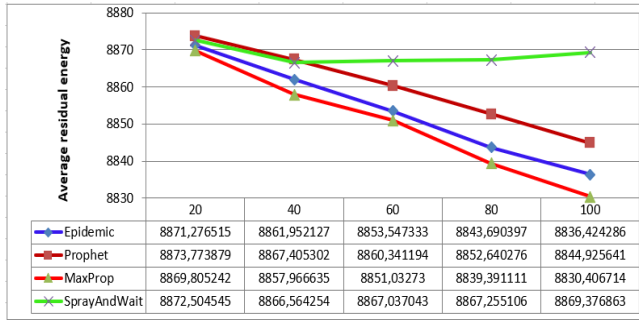


Figure 16. Average residual energy of solar DTN nodes evaluated on the MBM model and DTN protocols

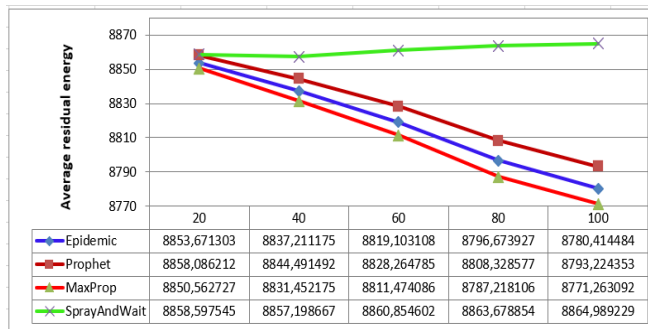


Figure 17. Average residual energy of solar DTN nodes evaluated on the SPMBM model and DTN protocols

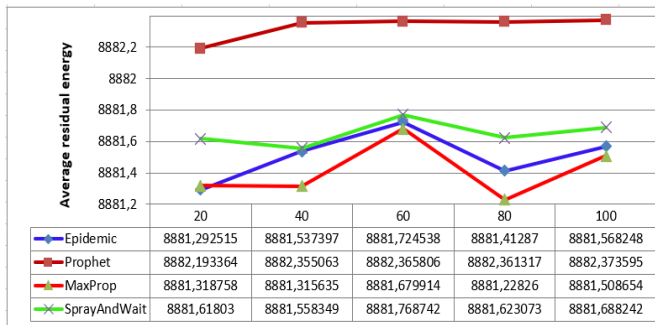


Figure 18. Average residual energy of solar DTN nodes evaluated on the RW model and DTN protocols

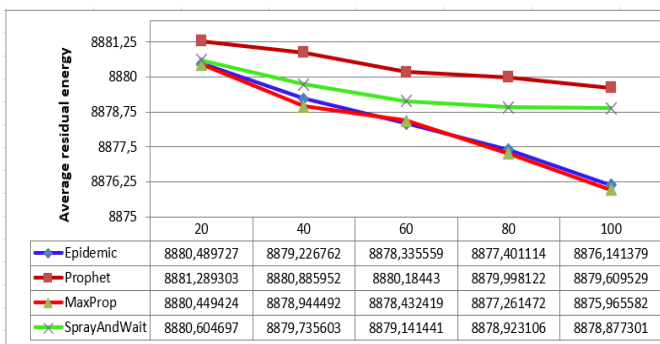


Figure 19. Average residual energy of solar DTN nodes evaluated on RWP model and DTN protocols

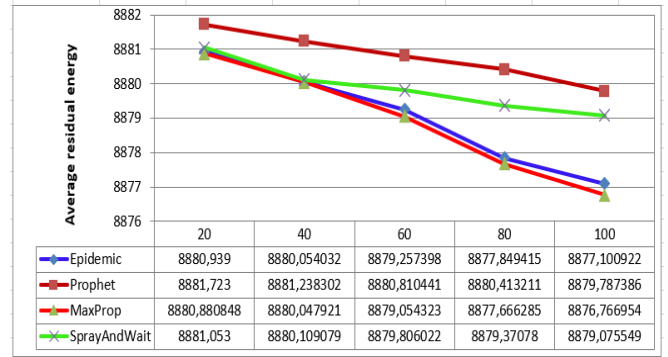


Figure 20. Average residual energy of solar DTN nodes evaluated on the RD model and DTN protocols

### 9.2.3 Impact of routing protocols

The protocols also influence energy consumption. Spray-and-Wait and Prophet stand out for their better energy efficiency, with Spray-and-Wait limiting transmissions through its restricted forwarding strategy, and Prophet optimizing recipient selection via probabilistic predictions. In contrast, MaxProp and Epidemic consume more energy. MaxProp incorporates complex priority management, while Epidemic increases consumption through multiple and redundant transmissions.

### 9.2.4 Impact of mobility models

The characteristics of mobility models play an important role in energy consumption. The MBM and SPMBM models, based on planned routes and maps, require more energy due to frequent transmissions to maintain connectivity. In contrast, the random RW, RWP and RD models, with unpredictable movements, reduce unnecessary transmissions, thereby reducing energy consumption.

## 9.3 Evaluation of the energy performance of ordinary DTN nodes using limited energy resources

In this section, we evaluate the energy performance of ordinary DTN nodes powered by limited energy resources. The evaluations consider different mobility models (MBM, SPMBM, RW, RWP, RD) as well as routing protocols (Epidemic, Prophet, Spray-and-Wait, MaxProp). Figures 21-25 illustrate the energy performance of ordinary DTN nodes based on the mobility models and routing protocols.

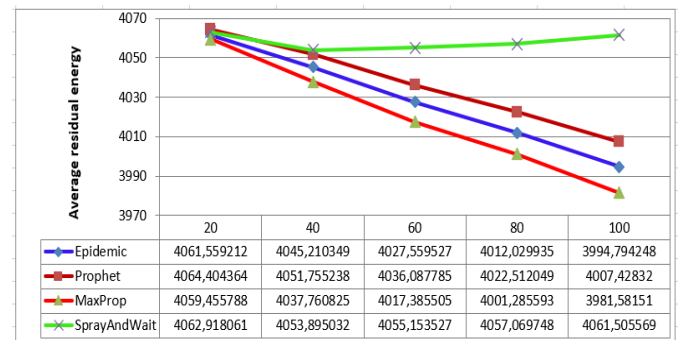


Figure 21. Average residual energy of ordinary DTN nodes evaluated on the MBM model and DTN protocols

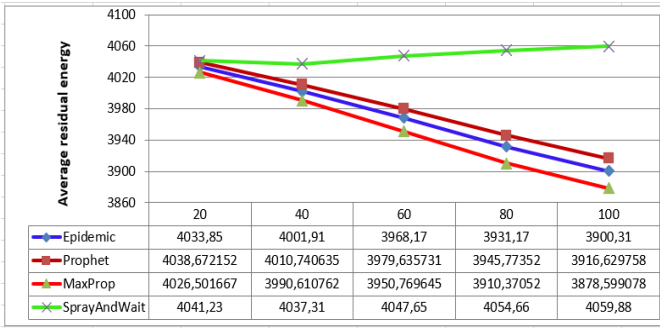


Figure 22. Average residual energy of ordinary DTN nodes evaluated on the SPMBM model and DTN protocols

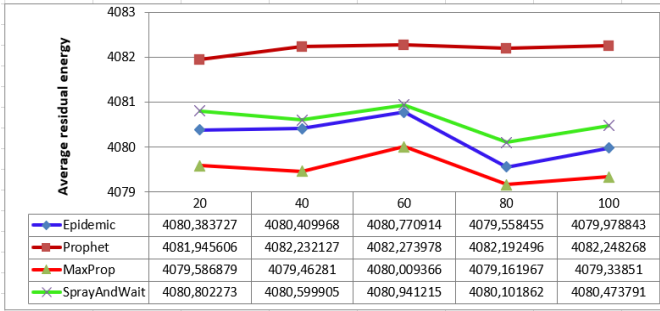


Figure 23. Average residual energy of ordinary DTN nodes evaluated on the RW model and DTN protocols

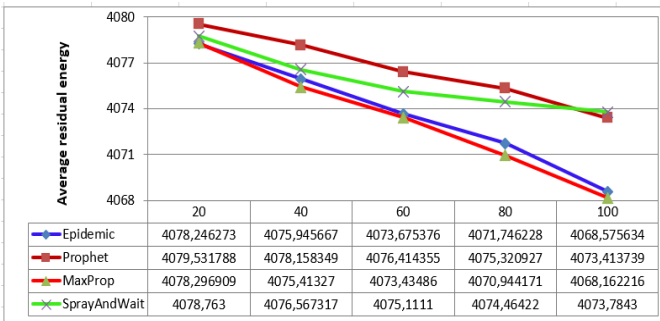


Figure 24. Average residual energy of ordinary DTN nodes evaluated on the RWP model and DTN protocols

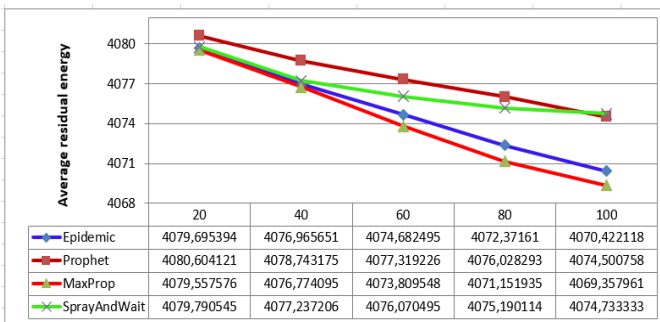


Figure 25. Average residual energy of ordinary DTN nodes evaluated on the RD model and DTN protocols

contrast, the MBM and SPMBM models show lower residual energies, with values of 4035.56761 Joules and 3986.22217 Joules, respectively.

### 9.3.2 Energy consumption

The energy consumption of DTN nodes is significantly impacted by the mobility models and protocols used. The random models RW, RWP, and RD exhibit relatively low energy consumption, reaching 718.275382 Joules, 720.905129 Joules, and 720.349807 Joules, respectively, due to the unpredictable nature of the movements. In contrast, the map-based models MBM and SPMBM, requiring complex trajectory calculations, show higher energy consumption, reaching 742.13414 Joules and 771.162075 Joules, respectively.

### 9.3.3 Impact of routing protocols

The routing protocols directly influence energy consumption. The Spray-and-Wait and Prophet protocols are distinguished by lower energy consumption, thanks to Spray-and-Wait's limited forwarding strategy and Prophet's use of probabilistic predictions. In contrast, the MaxProp and Epidemic protocols show higher energy consumption due to MaxProp's complex priority management mechanisms and the redundant transmissions characterizing the Epidemic protocol.

### 9.3.4 Impact of mobility models

The mobility models have a strong impact on energy consumption. The mobility models MBM and SPMBM consume more energy due to complex trajectories requiring more path calculations to maintain connectivity, which increases the frequency of encounters and transmissions. In contrast, the RW, RWP, and RD models result in lower energy consumption due to unpredictable movements (RW), periods of inactivity (RWP), and direction changes (RD), thereby limiting unnecessary transmissions.

## 10. SYNTHESIS OF EVALUATIONS

### 10.1 Residual energy and energy consumption of DTN nodes

The analysis of all results shows that the average residual energy of solar DTN nodes is significantly higher (approximately 8865,43469 Joules) compared to ordinary DTN nodes (approximately 4050,59244 Joules), despite an initial energy set at 4800 Joules. This difference is explained by the use of renewable energy resources by the solar DTN nodes. Moreover, the average energy consumption of solar DTN nodes is slightly lower (734,565307 Joules) compared to ordinary DTN nodes (749,40756 Joules), due to the absence of energy depletion in solar nodes. These observations are consistent across all the mobility models and DTN protocols studied.

### 10.2 Understanding the behaviors of DTN protocols and mobility models

The analysis of the energy performance of nodes in DTN networks, considering renewable and limited energy resources, reveals notable differences depending on the routing protocols and mobility models. The Spray-and-Wait and Prophet protocols stand out for their energy efficiency, while MaxProp

### 9.3.1 Residual energy

The analysis of the results indicates a decrease in the average residual energy compared to the initial energy of 4800 Joules. The random models RW, RWP, and RD retain greater residual energy levels, reaching 4080.62365 Joules, 4074.79848 Joules, and 4075.75028 Joules, respectively. In

is the least efficient.

In the context of map-based mobility models (MBM, SPMBM), the Spray-and-Wait protocol shows the best performance in terms of residual energy. In contrast, the MaxProp protocol is the least energy-efficient.

In the context of individual mobility models (RW, RWP, RD), the PROPHET protocol also proves to be more energy-efficient than the others, while MaxProp remains the most energy-consuming.

Moreover, nodes using map-based social mobility models (MBM, SPMBM) consume more energy than those with individual mobility models (RW, RWP, RD).

These results highlight the importance of selecting the appropriate protocols and mobility models to optimize the energy efficiency of DTN networks in environments with renewable or limited energy resources.

### 10.3 Optimization of DTN protocols and mobility models

Optimizing the choice of DTN protocols and mobility models, based on renewable or limited energy sources, is essential to maximize the performance of DTN networks.

Based on previous analyses and justifications, we can deduce the most energy-efficient combinations between mobility models and DTN routing protocols, taking into account renewable and limited energy resources, as well as residual energy and energy consumption by DTN nodes. These findings and conclusions are illustrated in Figures 26 and 27 and Table 8.

**Table 8.** Energy-efficient combinations between mobility model and DTN protocol for a solar DTN node and an ordinary DTN node

Energy Efficient Combinations		Average Residual Energy	
DTN Protocols	Mobility Models	Ordinary DTN Node	Solar DTN Node
Spray-and-wait	MBM	4058,10839	8868,54756
Spray-and-wait	SPMBM	4048,146	8861,06378
Prophet	RW	4082,1785	8882,32983
Prophet	RWP	4076,56783	8880,39347
Prophet	RD	4077,43911	8880,79447

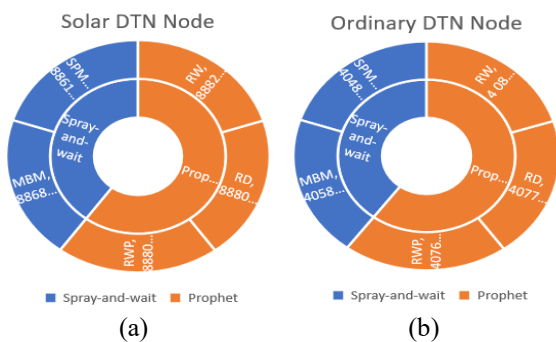


**Figure 26.** Energy-efficient combinations between mobility model and DTN protocol for (a) a solar DTN node and (b) an ordinary DTN node

Figure 26(a) and Figure 26(b) show the most energy-efficient combinations between mobility models and DTN protocols, based on average residual energy for a solar DTN node (a) compared to an ordinary DTN node (b).

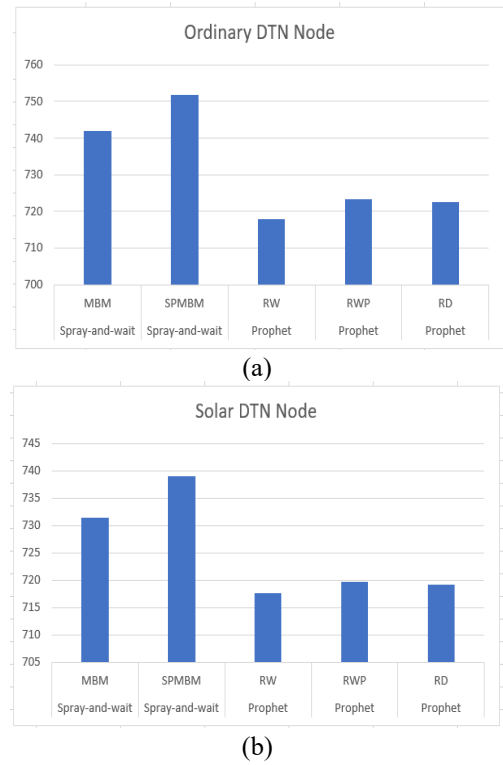


**Figure 27.** The most energy-efficient combinations between mobility models and DTN protocols, based on the average energy consumption by (a) ordinary DTN nodes and (b) solar DTN nodes

Figure 27(a) and Figure 27(b) show the most energy-efficient combinations between DTN protocols and mobility models, based on average energy consumption for an ordinary DTN node (a) compared to a solar DTN node (b).

Optimizing the choices of DTN protocols and mobility models in DTN networks is crucial to ensure maximum energy efficiency and reliable connectivity in diverse conditions and remote environments. This solar-based approach contributes to increasing the sustainability and reliability of DTN networks while enhancing the autonomy of nodes.

## 11. CONCLUSION

In conclusion, our research has focused on the energy challenges faced by DTN networks, especially in isolated and hard-to-reach environments. We have proposed a sustainable energy management approach aimed at mitigating routing problems and energy challenges associated with DTN nodes, by integrating solar energy into the architecture of DTN nodes to enhance their autonomy durability and performance. Our contributions include the complete modeling of an energy-autonomous solar DTN node, mathematical and stochastic modeling, as well as evaluations of the energy power generated by a solar DTN node in regular and random movement and orientation, simulations in the ONE simulator based on realistic scenarios involving solar DTN nodes, and in-depth evaluations of the impact of solar DTN nodes on the energy performance of DTN networks, considering various DTN protocols and mobility models.

The results of our simulations have revealed that solar DTN nodes exhibit a significantly higher average residual energy than ordinary DTN nodes, thereby validating and demonstrating the effectiveness of integrating solar energy

into DTN networks. The analysis of DTN protocols and mobility models has shown that social map-based mobility models (MBM, SPMBM) presented the highest energy consumption, compared to individual mobility models (RW, RWP, RD). The PROPHET and Spray-and-Wait protocols are energy-efficient, while the Epidemic and MaxProp protocols presented the highest energy consumption. Furthermore, we have identified the most energy-efficient combinations between mobility models and DTN protocols as follows: The Spray-and-Wait protocol exhibited compatibility with map-based social mobility models (MBM, SPMBM), while the PROPHET protocol showed alignment with individual mobility models (RW, RWP, RD).

Although focused on solar energy, this research opens promising perspectives for the optimization of DTN networks, particularly in resource-constrained environments. It highlights the importance of the choice of protocols and mobility models in energy efficiency. Future research could explore the use of hybrid energy sources and the integration of emerging technologies to enhance the autonomy and sustainability of DTN networks in diverse contexts.

## REFERENCES

- [1] Rodrigues, J.J., Soares, V.N. (2021). An introduction to delay and disruption tolerant networks (DTNs). In *Advances in Delay-Tolerant Networks (DTNs) (Second Edition)*. Woodhead Publishing, pp. 1-20. <https://doi.org/10.1016/B978-0-08-102793-6.00001-1>
- [2] Sammou, E.M. (2023). A hierarchical routing tree topology based on probabilistic selection of cluster head and super cluster head to overcome inter-cluster and intra-cluster routing problems in DTN networks. *Journal of Theoretical and Applied Information Technology (JATIT)*, 101(3): 1400-1410. <http://www.jatit.org/volumes/Vol101No3/33Vol101No3.pdf>.
- [3] Sammou, E.M. (2023). A social spray-and-wait routing protocol based on social nodes in delay tolerant networks (DTNs). *Journal of Theoretical and Applied Information Technology (JATIT)*, 101(6): 2385-2398. <http://www.jatit.org/volumes/Vol101No6/28Vol101No6.pdf>.
- [4] Sammou, E.M. (2012). Efficient probabilistic routing in delay tolerant networks. In *2012 International Conference on Multimedia Computing and Systems*, Tangiers, Morocco, pp. 584-589. <https://doi.org/10.1109/ICMCS.2012.6320290>
- [5] Pentland, A., Fletcher, R., Hasson, A. (2004). DakNet: Rethinking connectivity in developing nations. *Computer*, 37(1): 78-83. <https://doi.org/10.1109/MC.2004.1260729>
- [6] Grasic, S., Lindgren, A. (2014). Revisiting a remote village scenario and its DTN routing objective. *Computer Communications*, 48: 133-140. <https://doi.org/10.1016/j.comcom.2014.04.003>
- [7] Elewaily, D.I., Ali, H.A., Saleh, A.I., Abdelsalam, M.M. (2024). Delay/disruption-tolerant networking-based integrated deep-space relay network: State-of-the-art. *Ad Hoc Networks*, 152: 103307. <https://doi.org/10.1016/j.adhoc.2023.103307>
- [8] Ababou, M., Bellafkih, M., El kouch, R. (2018). Energy efficient routing protocol for delay tolerant network based on fuzzy logic and ant colony. *International Journal of Intelligent Systems & Applications*, 10(1): 69-77. <https://doi.org/10.5815/ijisa.2018.01.08>
- [9] Chowdhury, A., De, D., Raychaudhuri, A., Bakshi, M. (2023). Corrigendum to energy-efficient coverage optimization in wireless sensor networks based on voronoi-glowworm swarm optimization-k-means algorithm. *Ad Hoc Networks*, 139: 102907. <https://doi.org/10.1016/j.adhoc.2022.102907>
- [10] Olusesi, A.T., Olaniyan, O.M., Omodunbi, B.A., Wahab, W.B., Adetunji, O.J., Olukoya, B.M. (2023). Energy management model for mobile ad hoc network using adaptive information weight bat algorithm. *e-Prime - Advances in Electrical Engineering, Electronics and Energy*, 5: 100255. <https://doi.org/10.1016/j.prime.2023.100255>
- [11] Singh, A.K., Pamula, R., Srivastava, G. (2022). An adaptive energy aware DTN-based communication layer for cyber-physical systems. *Sustainable Computing: Informatics and Systems*, 35: 100657. <https://doi.org/10.1016/j.suscom.2022.100657>
- [12] Sammou, El Mastapha. (2024). Impact of renewable energy resources on the performance of DTN networks in the context of hierarchical routing tree topology (HRTT). *Procedia Computer Science*, 236: 185-193. <https://doi.org/10.1016/j.procs.2024.05.020>
- [13] Israr, A., Yang, Q., Li, W., Zomaya, A.Y. (2021). Renewable energy powered sustainable 5G network infrastructure: Opportunities, challenges and perspectives. *Journal of Network and Computer Applications*, 175: 102910. <https://doi.org/10.1016/j.jnca.2020.102910>
- [14] Ahmed, F., Naeem, M., Ejaz, W., Iqbal, M., Anpalagan, A. (2018). Resource management in cellular base stations powered by renewable energy sources. *Journal of Network and Computer Applications*, 112: 1-17. <https://doi.org/10.1016/j.jnca.2018.03.021>
- [15] Devela, N.R., Kandpal, T.C., Singh, B. (2024). A review of renewable energy based power supply options for telecom towers. *Environmental, Development and Sustainability*, 26: 2897-2964. <https://doi.org/10.1007/s10668-023-02917-7>
- [16] LetsGoDigital. (2019). Xiaomi Allegedly Designs a Phone with an In-Built Solar Panel. <http://nl.letsgodigital.org/smartphones/xiaomi-mobile-telefoon-solar-oplader/>.
- [17] Roy, R.R. (2011). Random walk mobility. In: *Handbook of Mobile Ad Hoc Networks for Mobility Models*. Springer, Boston, MA, pp. 35-63. [https://doi.org/10.1007/978-1-4419-6050-4\\_3](https://doi.org/10.1007/978-1-4419-6050-4_3)
- [18] Pramanik, A., Choudhury, B., Choudhury, T.S., Arif, W., Mehedi, J. (2015). Simulative study of random waypoint mobility model for mobile ad hoc networks. In *2015 Global Conference on Communication Technologies (GCCT)*, Thuckalay, India, pp. 112-116. <https://doi.org/10.1109/GCCT.2015.7342634>
- [19] Nain, P., Towsley, D., Liu, B., Liu, Z. (2005). Properties of random direction models. In *Proceedings IEEE 24th Annual Joint Conference of the IEEE Computer and Communications Societies.*, Miami, FL, USA, pp. 1897-1907. <https://doi.org/10.1109/INFCOM.2005.1498468>
- [20] Sammou, E.M. (2023). Performance evaluation of DTN routing protocols on map-based social mobility models for DTN networks. *Journal of Theoretical and Applied*

- Information Technology (JATIT), 101(22): 7339-7356. <http://www.jatit.org/volumes/Vol101No22/28Vol101No22.pdf>.
- [21] Keränen, A., Ott, J., Kärkkäinen, T. (2009). The ONE simulator for DTN protocol evaluation. In SIMUTools "09" Proceedings of the 2nd International Conference on Simulation Tools and Techniques, ICST, New-York, NY, USA, pp. 1-10. <https://doi.org/10.4108/ICST.SIMUTOOLS2009.5674>
- [22] Vahdat, A., Becker, D. (2000). Epidemic routing for partially-connected ad hoc networks. Technical Report CS-2000-06, Computer Science Department, Duke University, NC, Durham, USA.
- [23] Lindgren, A., Doria, A., Schelén, O. (2004). Probabilistic Routing in Intermittently Connected Networks. In: Dini, P., Lorenz, P., de Souza, J.N. (eds) Service Assurance with Partial and Intermittent Resources. Springer, Berlin, pp. 239-254. [https://doi.org/10.1007/978-3-540-27767-5\\_24](https://doi.org/10.1007/978-3-540-27767-5_24)
- [24] Spyropoulos, T., Psounis, K., Raghavendra, C.S. (2005). Spray-and-Wait: An efficient routing scheme for intermittently connected mobile networks. In Proceedings of the 2005 ACM SIGCOMM Workshop on Delay-Tolerant Networking. ACM Press, New York, pp. 252-259. <https://doi.org/10.1145/1080139.1080143>
- [25] Burgess, J., Gallagher, B., Jensen, D., Levine, B.N. (2006). MaxProp: Routing for vehicle-based disruption-tolerant networks. In Proceedings of the 25th IEEE International Conference on Computer Communications, Barcelona, Spain, pp. 1-11. <https://doi.org/10.1109/INFOCOM.2006.228>
- [26] Piovesan, N., Gambin, A.F., Miozzo, M., Rossi, M., Dini, P. (2018). Energy sustainable paradigms and methods for future mobile networks: A survey. Computer Communications, 119: 101-117. <https://doi.org/10.1016/j.comcom.2018.01.005>
- [27] Khernane, S., Bouam, S., Arar, C. (2024). Renewable energy harvesting for wireless sensor networks in precision agriculture. International Journal of Network and Distributed Computing, 12: 8-16. <https://doi.org/10.1007/s44227-023-00017-6>
- [28] Bouguera, T. (2019). Energy-autonomous communicating sensor for the IoT. Ph.D. dissertation. Department of Electronics, University of Nantes. <https://hal.science/tel-02092386>
- [29] Vodapally, S.N., Ali, M.H. (2023). A comprehensive review of solar photovoltaic (PV) technologies, architecture, and its applications to improved efficiency. Energies, 16(1): 319. <https://doi.org/10.3390/en16010319>
- [30] Ram, J.P., Babu, T.S., Rajasekar, N. (2017). A comprehensive review on solar PV maximum power point tracking techniques. Renewable and Sustainable Energy Reviews, 67: 826-847. <https://doi.org/10.1016/j.rser.2016.09.076>
- [31] Yang, Q., Huang, Y., Wu, Y., Wu, S. (2023). Improving lithium-ion battery performance with attapulgite nanoparticle-modified polypropylene separator. International Journal of Electrochemical Science, 18(12): 100324. <https://doi.org/10.1016/j.ijeoes.2023.100324>
- [32] Raut, K., Shendge, A., Chaudhari, J., Lamba, R., Alshammari, N.F. (2024). Modeling and simulation of photovoltaic powered battery-supercapacitor hybrid energy storage system for electric vehicles. Journal of Energy Storage, 82: 110324. <https://doi.org/10.1016/j.est.2023.110324>
- [33] Myers, D.R. (2013). Solar Radiation: Practical Modeling for Renewable Energy Applications (1st ed.). CRC Press, Boca Raton, Florida, USA. <https://doi.org/10.1201/b13898>
- [34] Duffie, J.A., Beckman, W.A. (2013). Solar Engineering of Thermal Processes (4th ed.). John Wiley & Sons, Inc. <https://doi.org/10.1002/9781118671603>
- [35] Luque, A., Hegedus, S. (2011). Handbook of Photovoltaic Science and Engineering. John Wiley & Sons, Ltd. <https://doi.org/10.1002/9780470974704>
- [36] Mihelić-Bogdanić, A., Budin, R., Filipan, V. (1996). Investigation of solar declination. Renewable Energy, 7(3): 271-277. [https://doi.org/10.1016/0960-1481\(95\)00135-2](https://doi.org/10.1016/0960-1481(95)00135-2)
- [37] Magadley, E., Kabha, R., Yehia, I. (2021). Outdoor comparison of two organic photovoltaic panels: The effect of solar incidence angles and incident irradiance. Renewable Energy, 173: 721-732. <https://doi.org/10.1016/j.renene.2021.04.021>
- [38] Paret, T.W., Wöhrbach, M., Buck, R., Weinrebe, G. (2020). Incidence angles on cylindrical receivers of solar power towers. Solar Energy, 201: 1-7. <https://doi.org/10.1016/j.solener.2020.02.077>
- [39] Obiwulu, A.U., Erusiafe, N., Olopade, M.A., Nwokolo, S.C. (2022). Modeling and estimation of the optimal tilt angle, maximum incident solar radiation, and global radiation index of the photovoltaic system. Heliyon, 8(6): e09598. <https://doi.org/10.1016/j.heliyon.2022.e09598>
- [40] Danandeh, M.A., Mousavi G., S.M. (2018). Solar irradiance estimation models and optimum tilt angle approaches: A comparative study. Renewable and Sustainable Energy Reviews, 92: 319-330. <https://doi.org/10.1016/j.rser.2018.05.004>
- [41] Xiao, Z., Gao, B., Huang, X., Chen, Z., Li, C., Tai, Y. (2024). An interpretable horizontal federated deep learning approach to improve short-term solar irradiance forecasting. Journal of Cleaner Production, 436: 140585. <https://doi.org/10.1016/j.jclepro.2024.140585>
- [42] Salazar-Peña, N., Tabares, A., González-Mancera, A. (2023). Sequential stochastic and bootstrap methods to generate synthetic solar irradiance time series of high temporal resolution based on historical observations. Solar Energy, 264: 112030. <https://doi.org/10.1016/j.solener.2023.112030>
- [43] Barbón, A., Carreira-Fontao, V., Bayón, L., Silva, C.A. (2023). Optimal design and cost analysis of single-axis tracking photovoltaic power plants. Renewable Energy, 211: 626-646. <https://doi.org/10.1016/j.renene.2023.04.110>
- [44] Fraunhofer Institute for Solar Energy Systems ISE. (2023). World Record: Efficiency Reached for Multi-Junction Solar Cells at Fraunhofer ISE. Fraunhofer ISE, accessed on Jan. 7, 2024.
- [45] Joseph, E., Singh, B.S.M., Ching, D.L.C. (2023). Developing a simple algorithm for photovoltaic array fault detection using MATLAB/Simulink simulation. International Journal of Energy Production and Management, 8(4): 235-240. <https://doi.org/10.18280/ijepm.080405>
- [46] Al-Azawiey, S.S., Mohamed, M.M., Arifin, A.B. (2023). Effectiveness of PV/T passive natural air cooling by backside attached fins. International Journal of Energy

Production and Management, 8(2): 55-62. <https://doi.org/10.18280/ijepm.080201>

[47] Hachicha, A.A., Abo-Zahhad, E.M. (2023). Dust effect on solar energy systems and mitigation methods. International Journal of Energy Production and Management, 8(2): 97-105. <https://doi.org/10.18280/ijepm.080206>

[48] Khezri, R., Mahmoudi, A., Aki, H. (2022). Resiliency-oriented optimal planning for a grid-connected system with renewable resources and battery energy storage. IEEE Transactions on Industry Applications, 58(2): 2471-2482. <https://doi.org/10.1109/TIA.2021.3133340>

[49] Song, C., Kawai, R. (2023). Monte Carlo and variance reduction methods for structural reliability analysis: A comprehensive review. Probabilistic Engineering Mechanics, 73: 103479. <https://doi.org/10.1016/j.probengmech.2023.103479>

[50] The ONE (2024). The Opportunistic Network Environment Simulator, Project Page of the ONE Simulator. <https://www.netlab.tkk.fi/tutkimus/dtn/theone>.

## NOMENCLATURE

### Acronyms

DTN	Delay-Tolerant Networks
RW	Random Walk
RWP	Random Waypoint
RD	Random Direction

MBM	Map Based Mobility
SPMBM	Shortest Path Map Based Mobility
ONE	Opportunistic Network Environment

### Symbols

$S_{time}$	Solar time
$S_{dec}$	Solar declination
$I_A$	Solar incidence angle
Long	Longitude
Lat	Latitude
$P_{generated}$	Generated power
$A_{panel}$	Solar panel dimension, m <sup>2</sup>
$E_{panel}$	Solar panel efficiency, %
G	Average solar irradiance, W/m <sup>2</sup>
$G_{hor}$	Solar horizontal irradiance, W/m <sup>2</sup>
$E_{St}$	Energy stored, joules
$T_{exp}$	Exposure time, seconds
$C_{DTN}$	Communication energy, joules
$P_{DTN}$	Communication Power, W
T	Communication activity time, seconds
$C_{transmission}$	Transmission energy, joules
$P_{transmission}$	Transmission power, W
$T_{transmission}$	Transmission time, seconds
$C_{reception}$	Reception energy, joules
$P_{reception}$	Reception power, W
$T_{reception}$	Reception time, seconds
$C_{search}$	Search energy, joules
$P_{search}$	Search power, W
$T_{search}$	Search time, seconds